Theoretical Analysis and Design of a High Bandwidth SiNx on SOI Grating Coupler for Telecommunications Application

Albert Djikeng

albert.djikeng@yahoo.com
Department of Electrical and Computer Engineering
University of Texas at San Antonio

Mehdi Shadaram, PhD

mehdi.shadaram@utsa.edu
Department of Electrical and Computer Engineering
University of Texas at San Antonio

***Abstract*— One fundamental building block of integrated photonics is the fiber-to-chip grating coupler. The grating coupling method is mainly hindered by the vast difference in mode areas between the fiber cable and the waveguide, which causes low coupling efficiency. Other challenges include limited bandwidth, backward scattered light, and mode mismatch. Couplers based on a silicon nitride (SiN_x) material platform can achieve wider bandwidths and better coupling efficiency than silicon-based couplers. In this research, we identify methods to increase the 1dB optical bandwidth of a SiN_x on silicon-on-insulator (SOI) grating coupler while maintaining a coupling efficiency greater than 40% in efforts to develop a high-capacity grating coupler for telecommunications applications. Methods such as asymmetric grating trenches for low back reflections and optimization of grating dimensions are examined. The optimized structures yielded results up to 28.57 nm for 1dB bandwidth and a maximum coupling efficiency of 49.77%.**

Keywords: *Photonics, fiber optics communications, grating coupler, photonic integrated circuits*

I. INTRODUCTION

Grating couplers provide the most practical method for guided mode resonance when attempting to couple optical signal from a fiber cable to an on-chip photonic waveguide. Their major advantages include high alignment tolerance and a simple fabrication process; which provide for wafer-scale automated testing. The light can be coupled in at any arbitrary location on the chip, which allows for out-of-plane coupling (shining the light at an angle incident to the device). Grating couplers also use diffraction gratings, along the surface of the top substrate, to couple a near incident fiber-mode to the waveguide mode. The typical design contains periodic 10μm x 10μm trenches which are often curved to help focus the optical signal into the waveguide and reduce the need for polarization or tapper structures. The main disadvantage of grating couplers are their limited bandwidth and relatively low coupling efficiency; the former due to their typical design for the center wavelength of single mode fibers, and the latter due to backward scattered light, diffraction, and mode mismatch. Previous chip-to-fiber coupling research [7] has identified that a SiN_x layer on the SOI substrate (fig. 1) can achieve wider bandwidths than solely silicon-based SOI platforms. While they are still challenging to implement, grating couplers offer less costly and greatly simplified alternatives for fiber-to-chip coupling.

II. Problem Statement

Nanophotonic waveguides and components have become ubiquitous for use in the large-scale integration of photonic integrated circuits (PICs), and as a result, coupling light between nanophotonic waveguides and a single-mode fiber is a relevant issue. Materials with a high refractive index contrast are useful for high-

density photonic integrated circuits; however, the difficulty lies in the size disparity between optical fibers and integrated waveguides. The coupling problem is best addressed with a surface coupler that can be placed anywhere on a chip, does not require polishing of facets, and allows for wafer-scale testing by coupling light in and out of the surface of the chip. Waveguide grating couplers are suitable for this task. However, when conventional gratings with a small coupling strength are used, long gratings are needed, and the out-coupled beam is much larger than the fiber mode. As a result, an additional lens is needed to couple to a fiber or, alternatively, a curved grating can be used to focus the light into a fiber [6]. In this research, we demonstrate an approach employing non-uniform gratings that allows for increased optical bandwidth and reduction in complexity of coupler fabrication, while also maintaining a relatively high coupling efficiency. Our design is inspired by a variety of bandwidth behavior as a function of both grating coupler intrinsic properties and fiber parameters such as position, beam waist and numerical aperture. Through the derivation of the rigorous bandwidth formula and investigation of the effects of individual parameters on bandwidth behavior, Zhe's research was able to propose several practical guidelines for grating coupler design and fiber operation in order to achieve wideband performance.

Our unique approach lies in the utilization of non-uniform gratings and a SiNx overlay to observe the effects of grating height and fill factor on 1dB bandwidth without the use of genetic equations or complex fabrication schemes. The specific structures proposed provide a means to more effectively redirect diffracted modes into the fundamental mode through gradual alteration of the doping concentrations from one end of the coupler to the other, thus lowering the mode mismatch between the fiber cable and the coupler input, as well as the coupler output and the on-chip waveguide. This theory has led to the development of three distinct designs (Base Case, Case 1, and Case 2) which all incorporate optimized dimensions. Based on this methodology, we present simulated results of a SiNx fiber-to-chip coupler. The coupler is designed with Lumerical FDTD and prospective fabrication would include only a single-step lithography process.

III. Applications of Research

The applications of this research are predominantly evident within telecommunications, more specifically fiber optic communications. Grating couplers are vital for the large-scale integration of photonic circuits due to the immense size disparity between photonic waveguides and

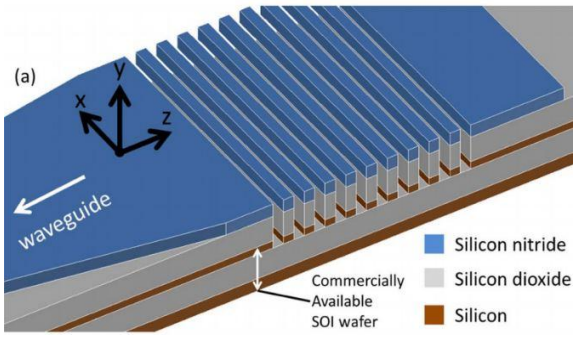

Fig. 1 Physical layout of SiN_x on SOI grating coupler [7]

fiber optic cables. The enhancement of integrated silicon photonics is the overall practical application for research in grating couplers. This enhancement has the potential to lead to significant improvements from data transfer speeds in communications to increased multi-core processor performance in the computer electronics industry. The grating design that allows for high bandwidth fiber-to-chip coupling in this research will contribute to current advancements in fiber optic communications. The surface coupling approach overcomes those limitations by utilizing waveguide gratings to diffract light into the waveguide (fig. 2). The inherent advantages in the packaging of the surface coupling approach have attracted many researchers worldwide to work on improving the performance of waveguide grating couplers [1]. The need for high-speed and energy-efficient interconnects for computing also drives research in grating couplers. Power and heat dissipation are the key limiting factors in regards to the increasing data rate required from electrical interconnects in modern multi-core microprocessors. The photonic technologies developed on SOI wafers can also be directly used in the integration of photonic structures on CMOS silicon wafers. This unification will allow the standardized large-volume fabrication capability of CMOS to be employed in the monolithic integration of photonics with high-speed electronic circuits. Thus, sophisticated optical communication and optical sensing systems on a single chip could soon be a reality.

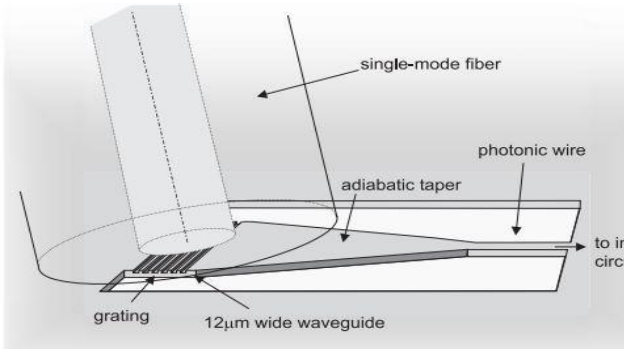

Fig.2 Principle of grating coupling for coupling between optical fiber cable and photonic waveguide [6]

IV. Methodology

Most of the emphasis on previous research has been put on increasing coupling efficiency [2] [3][10-11], not bandwidth. The focus of our research is to identify and optimize parameters to increase optical bandwidth while maintaining a fairly balanced coupling efficiency. The primary approach taken in this research is the usage of a SiNx top substrate and non-uniform grating structures with differing etching depths and fill factors. The three proposed designs are visualized in fig. 3. The low mismatch between the refractive index of the SiN_x and the effective index of the glass fiber helps dramatically reduce reflections at the fiber facet. For standard SOI uniform grating couplers, the effective index of the grating trenches (n_{eff}) can be expressed as

$$n_{eff} = F \cdot n_0 + (1 - F) \cdot n_E \qquad \textit{Eq.1}$$

where *F* is fill factor, and n_0 and n_E are the effective indices of the original silicon slab and the etched areas respectively. The periodic change in refractive index of the grating trenches enables the diffraction of the fundamental mode propagation in the silicon waveguide into free space [8]. The first order Bragg condition for grating periodicity (Λ) [2] gives us

$$\Lambda = \frac{\lambda_0}{neff - \sin(\theta)} \qquad \textit{Eq.2}$$

where λ_0 is the coupling-wavelength, θ is the angle between the fiber axis and the surface normal and n_{eff} is the effective refractive index of the top substrate (SiNx). For the pitch $\Lambda_{0,}$ which represents the difference between two gratings, we employ eq.3 [8] below.

$$\Lambda_0 = \frac{\lambda}{neff - \sin(\theta)(ncladding)} \qquad \textit{Eq.3}$$

Both grating period and pitch remain constant for all 3 active simulations within respective cases, but change slightly from case to case. Apodization is not performed in this experiment, but such method could be calculated using eq.4 [8]

$$F = F_0 - R \cdot z \qquad \textit{Eq.4}$$

where F_o is the initial fill-factor of the first radiative unit (SiNx), R is the linear apodization factor, and z is the distance of each radiative unit from the starting point of the grating. The grating coupler is typically regarded as a structure that transforms a surface wave into one or more leaky waves (space-harmonic fields) into top cladding and buried oxide (BOX) layer. To calculate the 1dB bandwidth, 3 main equations are considered. The first of which is the 1dB bandwidth coefficient (C_{1dB}) expressed as

$$C_{1dB} = \frac{\lambda}{2\pi w_1} \cdot \sqrt{\frac{\ln(10)}{5} + 2\ln\left(\frac{C_{\text{erf}}}{C_{\text{erf}}|b=0}\right)} \qquad \textbf{Eq. 5}$$

where λ_0 is the center wavelength (1550 nm). This proves that C_{1dB} should not be a constant, but rather determined by both the fiber and grating parameters [18]. With this, we can then compute the 1dB wavelength variation using

$$\Delta\lambda_{dB} = \frac{1}{\left|\frac{1}{\Lambda_0} - \frac{dn_w(\lambda_0)}{d\lambda}\right|} \cdot C_{1dB} \qquad \textbf{Eq. 6}$$

2.1 Grating Structure Design

The proposed grating coupler is based on a commercially available standard SOI wafer with a buried silicon layer thickness of 220 nm and a 2 μm buried oxide layer (BOX). For the Base Case, the following parameters are used: a SiNx thickness of 200 nm, a grating fill factor of 0.5, grating period (Λ) of .5, and a pitch of .5 ($\Lambda_{0,}$). The refractive indices of silicon, SiO2, and SiNx are 3.42, 1.9896, and 1.4431, respectively. These values are initially obtained by utilizing equations 1-4. There was no use of an overlay substrate on top of the SiNx top layer, therefore the refractive indices per grating altered between air and the specific refractive index of each respective grating. For Case 2 and Case 3, the optimized Base Case design is used as a foundation, and thus individual parameters are changed to observe their direct impact on optical bandwidth (grating height for Case 1 and fill factor for Case 2). Each design is depicted in fig. 3.

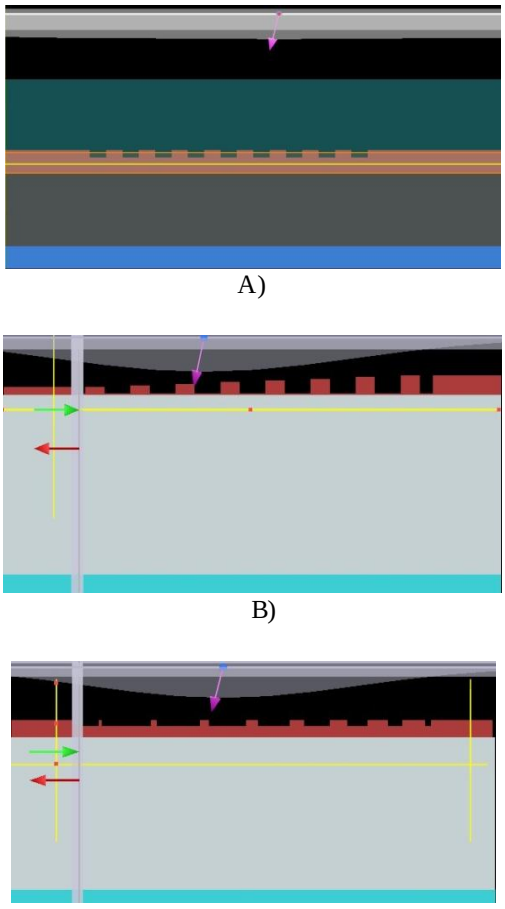

Fig. 3 Grating structure designs. A) Base Case, B) Case 1, C) Case 2. All designs are specified for a center wavelength (λ) of 1550 nm.

2.2 Detailed Approach

We begin with a basic 3-layer substrate composed of Si, SiO_2, and SiN_x (the proposed SiN_x on SOI platform). This platform will be referred to as the Base Case, to which the remaining 2 grating couplers will be compared. We will refer to parameter values acquired through equations (eq.1 and 2) and previous research as *calculated*, those obtained through parameterization sweeps as *parameterized*, and those obtained through optimization sweeps as *optimized* values. The parameters considered are listed in tables 4.1 – 4.3. Other parameters are held at constant values similar to those used in previous research [4][6-7][10] for all cases, with the exception of etching depth and fill factor (the two independent variables whose impact on optical bandwidth will be examined).

We first perform an active simulation on Lumerical FDTD utilizing the *calculated* parameter values listed in tables 4.1-4.3. We then run a parameter sweep to identify the best values for each parameter by analyzing the optical power transmission per wavelength. The active simulation is repeated (utilizing *parameterized* values) to verify and increase in optical transmission. The final step for the Base Case is to run an optimization simulation to identify even more precise measurements for the parameters. The optimization sweep gives results in the form of respective parameter values which yielded the highest average coupled power within the 200 nm wavelength spectrum. We are also able to acquire electromagnetic field intensity and the angular distribution of the emission; all as a function of wavelength. Thereafter, we run one last active simulation to verify that there is in fact an increase in transmission with the optimized parameters, compared to the results yielded utilizing *calculated* and *parameterized* values. Once the optimum parameter values are obtained for the Base Case, we implement Case 1 (utilizing the optimized Base Case structure as a foundation) by varying the etching depth to alter the height of the gratings; thus changing the structure of the. The optimum etching depth value acquired from the Base Case optimization is used to define the height of the center grating. All gratings to the left the center grating linearly decrease in height and those to the right linearly increase in height. This forms a grating structure analogous to a negative slope, as the etching depth increases from left to right of the coupler (fig. 3(B)). We repeat the simulation steps performed in the Base Case to obtain and verify the accuracy of the optimum parameter values. We then conduct an analysis of the effects of grating height/etching depth on the bandwidth of the SiNx coupler through direct comparison of the optical transmission and angular distribution results from the Base Case and Case 1. Next, we repeat the methodology for Case 2 (also utilizing the optimized Base Case structure as a foundation), in which case we alter the horizontal thickness of the gratings from left to right (fig. 3(C)). This is done in a similar fashion to the grating height variation in Case 1, whereby the horizontal thickness is increased from left to right. It is important to note that this causes a slight increase in the total length of the coupler, which is required to maintain a constant grating period. The optimum fill factor value acquired from the Base Case optimization is used to define the horizontal thickness of the center grating. All gratings to the left the center

grating linearly decrease in thickness and those to the right linearly increase in thickness. We once again repeat the simulation steps from the Base Case to obtain and verify the accuracy of the optimum parameter values. Subsequently, we conduct an analysis of the effects of fill factor on the bandwidth of the SiNx coupler through direct comparison of the optical transmission results from all 3 cases.

Table 4.1 List of grating parameter values for the Base Case

Name	Type	Value	Unit
Index	Number	1.44	
Material	Material	SiNx	
Target Length	Length	4	µm
h total	Length	0.22	µm
Etch Depth	Length	0.07	µm
Duty Cycle	Number	0.5	
Pitch	Length	0.5	µm
Input Length	Length	41	µm
Output Length	Length	13.25	µm

Table 4.2 List of grating parameter values for the first grating of Case 1. Each subsequent grating height (h total) is increased by .01875µm

Name	Type	Value	Unit
Index	Number	1.44	
Material	Material	SiNx	
Target Length	Length	.5	µm
h total	Length	0.08875	µm
Etch Depth	Length	0.07	µm
Duty Cycle	Number	0.59753	
Pitch	Length	0.57117	µm
Input Length	Length	1.2185	µm
Output Length	Length	0	µm

Table 4.3 List of grating parameter values for the first grating of Case 2. Each subsequent grating fill factor (duty cycle) is increased by .1µm

Name	Type	Value	Unit
Index	Number	1.44	
Material	Material	SiNx	
Target Length	Length	.5	µm
h total	Length	0.22	µm
Etch Depth	Length	0.07	µm
Duty Cycle	Number	0.1	
Pitch	Length	0.57117	µm
Input Length	Length	1.2185	µm
Output Length	Length	0	µm

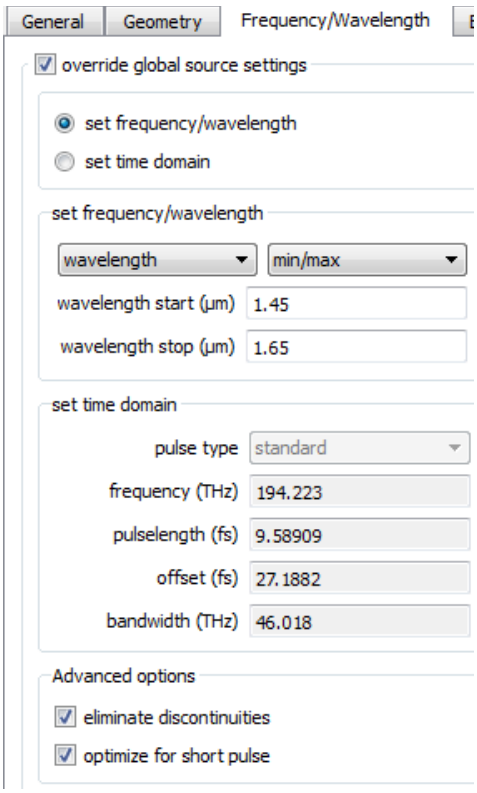

Fig. 4 List of fiber characteristic settings for all cases

There are a total of 9 active simulations (3 per case) and 6 sweeps (2 per case) performed within this experiment; including optimization and parameter sweeps. For the Base Case, we begin with the structure in fig. 3(A) which contains 3 layers, 8 gratings, an FDTD port (serves as planar light source), and a Gaussian beam source positioned .225um above the gratings at an angle of 13.9. We define *Coupled Power* as the determining indirect measurement for the total optical transmission as a function of all wavelengths within the 1.45nm-1.65nm span. The direct measurement is obtained through a DFT monitor placed at the output of the coupler. For Case 1, we manually set boundary ranges for the height of each of the 8 gratings to ensure that the "rising slope" structure is maintained as the grating height increases from left to right of the coupler. For Case 2, we manually set boundary ranges for the fill factor (horizontal thickness) of each of the 8 gratings to ensure that the structure is also maintained as the grating thicknesses increase from left to right of the coupler. For all parameter sweeps, 11 points are chosen. For all optimization sweeps, number of maximum generations was set to 50, with a generation size of 10. These properties are directly customizable and their values were chosen through calculations using equations in the results below.

V. Results

The data for this research was acquired through the 3-step process mentioned in section 2.2 of the methodology portion of this paper. For each case, we first ran the active simulation for the calculated values of the coupler. We then ran a parameter sweep to obtain the best values for each parameter per wavelength and obtained both calculated and direct measurements of total coupled optical power. The calculated measurements were obtained by using eq. 2 and the direct measurements were obtained through readings of a mode expansion monitor at the output of the coupler. Subsequently, we performed an optimization sweep to obtain the best values for all parameters in terms of average transmission for the entire 200 nm wavelength spectrum (1450 nm – 1650 nm). One last active simulation was performed to verify the accuracy of the optimum parameter values. It is important to differentiate between *parameterized* and *optimized* simulations. The *parameterized* simulations are used to obtain the best value (within a specified range), determined by the coupled optical power per wavelength, for each specific parameter. The resulting values from these simulations are listed in tables 5.1, 5.2, and 5.3, for the three cases respectively.

Table 5.1 Best values for grating dimensions from *parameterized* simulation of Base Case

Parameter	Peak Value
Fiber Angle	2.00353°
Etching Depth	0.0917078 (μm)
SiNx Thickness	0.27874 (μm)
Buried Si Thickness	0.21578 (μm)
Grating Length	1.15252 (μm)

Table 5.2 Best values for all gratings from *parameterized* simulation of Case 1

Parameter	Grating Height Peak Value (μm)
Grating 1	0.0840789
Grating 2	0.106513
Grating 3	0.125263
Grating 4	0.144013
Grating 5	0.162763
Grating 6	0.181513
Grating 7	0.200263
Grating 8	0.219013

Table 5.3 Peak values for all gratings for *parameterized* simulation of Case 2

Parameter	Fill Factor Peak Value (μm)
Grating 1	0.0668421
Grating 2	0.163158
Grating 3	0.263158
Grating 4	0.363158
Grating 5	0.463158
Grating 6	0.563158
Grating 7	0.663158
Grating 8	0.763158

The *optimized* simulations are used to obtain the best value (also within a specified range), determined by the average coupled optical power for all wavelengths within the 200 nm span, for each specific parameter. The resulting values from these simulations are listed in tables 5.4, 5.5, and 5.6, for the three cases respectively. Case 1 proved to be the best design, as it exhibited a 1dB bandwidth of 28.57 nm while maintaining a significantly larger coupling efficiency (49.7%) compared to the other two coupler designs. The results for each case are also discussed further in the next section.

Table 5.4 Best values for grating dimensions from *optimized* simulation of Base Case

Parameter	Peak Value
Fiber Angle	2.00353
Etching Depth	0.0917078 (μm)
SiNx Thickness	0.27874 (μm)
Buried Si Thickness	0.21578 (μm)
Grating Length	1.15252 (μm)

Table 5.5 Best values for all gratings from *optimized* simulation of Case 1

Parameter	Grating Height Peak Value (μm)
Grating 1	0
Grating 2	0.0927585
Grating 3	0.109955
Grating 4	0.12625
Grating 5	0.152305
Grating 6	0.167521
Grating 7	0.192261
Grating 8	0.218487

Table 5.6 Peak values for all gratings for *optimized* simulation of Case 2

Parameter	Fill Factor Peak Value (μm)
Grating 1	0.0892684
Grating 2	0.199289
Grating 3	0.200808
Grating 4	0.300518
Grating 5	0.495503
Grating 6	0.515778
Grating 7	0.629382
Grating 8	0.780995

For the Base Case, the initial active simulation showed boundary values of 3.88% and 2.45% with a peak of 3.67% at the 1550nm center frequency. To get the average coupled power for the entire wavelength spectrum, we calculated the average of the three measurements of coupled power for the respective wavelengths. This number is representative of the coupling coefficient (C_{1dB}) detailed in eq.7. After we obtain C_{1dB} we can now

measure the optical bandwidth of the grating coupler using Eq.8. With 200 nm for $d\lambda$, 1.9894 for $dn_w(\lambda_0)$, and 0.5 for Λ_0, $\Delta\lambda_{1dB}$ is found to be 20.900 nm. The same method is repeated for Cases 1 and 2. Tables 5.7, 5.8, and 5.9 show these calculations for the Base Case, Case 1, and Case 2.

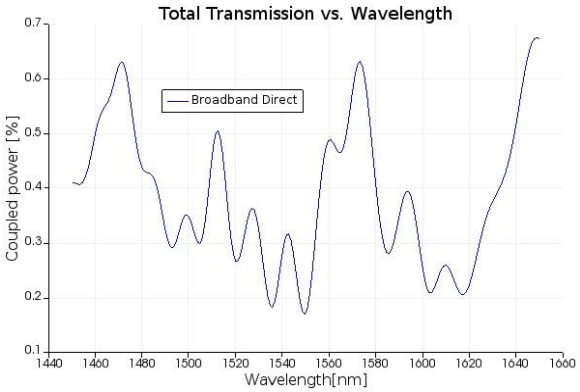

Fig. 5 *Optimized* simulation of average transmission as function of wavelength for Base Case

Table 5.7 1dB optical bandwidth for all simulations in Base Case

Measurement	$\frac{1}{\left\lvert\frac{1}{\Lambda_0}-\frac{dn_w(\lambda_0)}{d\lambda}\right\rvert}$	C_{1dB}	1dB Optical Bandwidth ($\Delta\lambda_{1dB}$)
Calculated	0.503	3.33	**1.675 nm**
Parameterized	0.503	41.55	**20.900 nm**
Optimized	0.503	41.55	**20.900 nm**

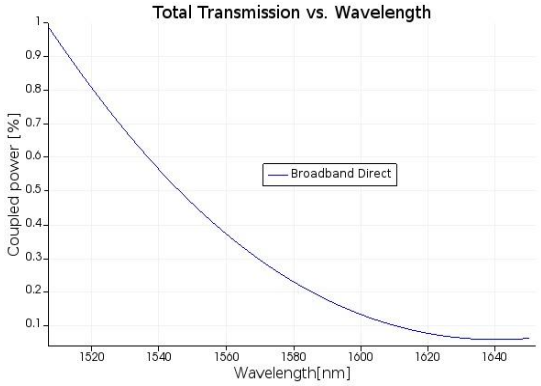

Fig. 6 *Optimized* simulation of average transmission as function of wavelength for Case 1

Table 5.8 1dB optical bandwidth for all simulations in Case 1

Measurement	$\frac{1}{\left\lvert\frac{1}{\Lambda_0}-\frac{dn_w(\lambda_0)}{d\lambda}\right\rvert}$	C_{1dB}	1dB Optical Bandwidth ($\Delta\lambda_{1dB}$)
Calculated	0.574	2.9	**1.66 nm**
Parameterized	0.574	48.67	**27.94 nm**
Optimized	0.574	49.777	**28.57 nm**

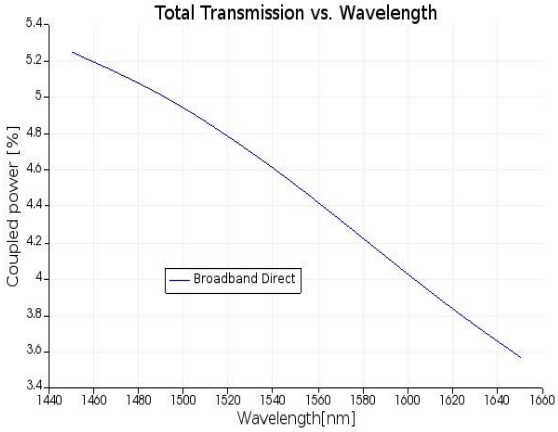

Fig. 7 *Optimized* simulation of average transmission as function of wavelength for Case 2

Table 5.9 1dB optical bandwidth for all simulations in Case 2

Measurement	$\frac{1}{\left\lvert\frac{1}{\Lambda_0}-\frac{dn_w(\lambda_0)}{d\lambda}\right\rvert}$	C_{1dB}	1dB Optical Bandwidth ($\Delta\lambda_{1dB}$)
Calculated	0.574	5.08	**2.92 nm**
Parameterized	0.574	44.88	**25.76 nm**
Optimized	0.574	44.4671	**25.52 nm**

VI. Discussion

The results obtained through this research confirmed the two. The first hypothesis was in regards to non-uniform SiNx gratings yielding a higher 1dB bandwidth compared to uniform SiNx gratings. This was confirmed by values obtained from the active simulations utilizing the *calculated* values (tables 5.7, 5.8, and 5.9) for each case. The Base Case calculated simulation yielded a 1dB bandwidth of 1.675 nm, while Case 1 yielded 1.66 nm, and Case 2 yielded 2.92 nm. This trend proves that using non-uniform grating structures do in fact increase the 1dB Bandwidth of SiNx couplers. The second hypothesis was in regards to the optimization methodology to identify the best values for all of the considered parameters of the grating coupler. This was confirmed by values obtained from the active simulations utilizing the *parameterized* (5.1, 5.2, 5.3) and *optimized* (5.4, 5.5, 5.6) values for each case. For the Base Case the active simulation utilizing the *parameterized* and *optimized* values yielded a 1dB bandwidth 20.900 nm, compared to the 1.675 nm obtained from the calculated simulation. Case 1 followed a similar trend, as the active simulation utilizing the *parameterized* parameter values yielded a 1dB bandwidth of 27.94 nm and the *optimized* simulation yielded a 1dB bandwidth of 28.57 nm; compared to the 1.66 nm obtained from the calculated simulation. The trend observed in Case 2 was similar to the Base Case and Case 1, with the exception of the parameterized simulation yielding a marginally higher 1dB bandwidth (25.76 nm) than that of the optimized simulation (25.52 nm). The reason for this is unknown, but the two results still showed a substantial improvement compared to the 2.92 nm 1dB bandwidth obtained from the active simulation utilizing the calculated parameter values in Case 2. The main challenge we faced was achieving high 1dB bandwidths to the likes of previous research (65 nm and 40 nm [7] [6]) that we based our Base Case design and optimization methodology on. The highest optical bandwidth obtained in this research was 28.57 nm, seen in the *optimized* design simulation of Case 1. The reasons for this relatively low 1dB bandwidth may include not using a polysilicon overlay, a non-optimal Base Case structure design, and SiNx on SOI limitations. Previous research [6] has shown that the easiest way to increase the coupling efficiency of a grating coupler with a regular silicon top layer is to put a polysilicon overlay cladding layer onto the silicon. This layer was shown to increase the up/down ratio of the out-coupled power. This method has not been conducted on SiNx couplers, but could potentially increase the coupling efficiency far above the 49.77% obtained in this research (*optimized* Case 1 structure). In such experiments, the refractive index of the overlay would have to be equal to the effective index of the fiber, to avoid reflections at the fiber facet. It should be noted that the coupling angle may change with the addition of a polysilicon overlay. In previous research [6], there was a 2 degree decrease in fiber angle (from 10° with no polysilicon overlay to 8° with the overlay) required to maintain the central wavelength at around 1550 nm. Another limitation of the maximum 1dB bandwidth achieved in this research could reside in the initial *calculated* parameter values for the Base Case. All values, with the exception of the four obtained from equations 1-4, were obtained from previous research [7-10]. Parameters such as grating length, buried SiO_2 thickness, input/output waveguide width/length, and fiber x-position, along with light source parameters shown in fig 4 were held constant throughout all 3 cases, but could be optimized to increase bandwidth results. A final prohibiting factor within this research is the inherent limitations of the SiNx on SOI platform, specifically the refractive index disparity between the glass fiber (1.5), SiNx gratings (2), and buried SiO_2 substrate (3.5). The mode mismatch issue was addressed in Cases 2 and 3 whereby the change in grating height and fill factor resulted in an increase of refractive index of each grating from left to right. The idea was to alter the doping

concentration and carrier densities of each grating, so that the change in refractive index per grating and air increased linearly from left to right. Thus, the left side of the coupler (where the light source is placed) would match the mode of the glass fiber and the right side of the coupler would match the mode of the Si on chip waveguide. This method worked, as Case 1 yielded the best results because this change in refractive index was more significant with a change in grating height compared to a change in fill factor. It also helped justify the trends in increasing 1dB bandwidth from calculated to optimized simulations within each case and from case 1 to case 2. Despite this success, the selection of a material with a much lower refractive index could help lower the mode mismatch even further and enhance the grating directionality of the coupler, which would reduce power leakage to the SOI substrate. A related point to note is that all imaginary refractive index values for the SiNx material created in the FDTD simulation were assumed to be 0, which may have also negatively impacted the individual refractive indices of the gratings in Cases 1 and 2. Despite not being able to obtain results seen in previous research (in terms of magnitude of 1dB bandwidth), we were able to identify the effects of change in grating height and etching depth on the optical bandwidth of a SiNx based grating coupler. The values obtained in tables 5.7, 5.8, and 5.9 also show that there is a dramatic increase in 1dB bandwidth from the *calculated* designs to the *parameterized* and *optimized* designs of the couplers in all 3 cases; thus confirming our unique non-uniform grating design approach and optimization methodology.

VII. Future Works

This research could be advanced by incorporating other grating structures (e.g. sinusoidal, saw-tooth) and substrates (e.g. InP, GaAs, Graphene) to modify the top layer of the grating. A 3D FDTD simulation may be also be performed to achieve more accurate results, as 3D simulations take into account an array of external factors that are not considered in the 2D simulation. For the 3D simulation, the pitch, duty cycle, and fiber alignment determined from the 2D simulation can all be used, along with circular etched lines to focus the optical signal into the waveguide. The design of the taper section of the 3D simulation can be parameterized to identify the best shape to use (e.g. straight, parabolic, etc.). Subsequently, the performance of the coupler within larger scale circuits (such as a full photonic link) could also be modeled through an INTERCONNECT simulation as visualized in figure 8.1 below. For this stage, the coupler S-parameters could be extracted from the 2D or 3D simulations and utilized as black box elements in the schematic representation of the circuit in INTERCONNECT. The design of an entire photonic circuit can also be pursued, with the integration of the grating coupler, and the fabrication of such chip could be done utilizing the method detailed in chapter 7 of this paper.

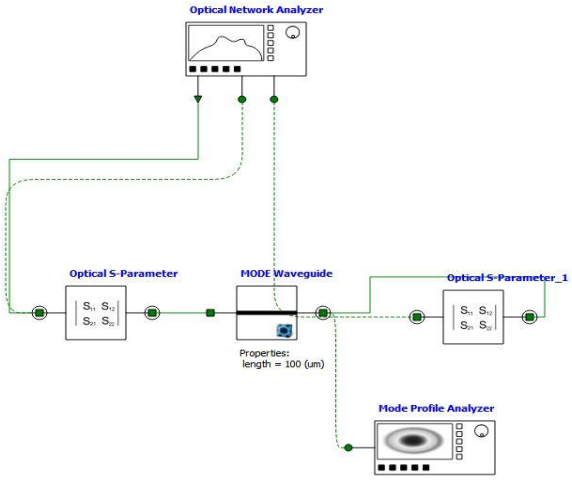

Fig.8 Schematic of a potential INTERCONNECT photonic link using exported S-parameters as grating coupler elements, along with an optical waveguide and analyzers to monitor the transmission of the optical signal

VIII. Conclusion

In conclusion, we have proposed and experimentally demonstrated a new design scheme of high-efficiency grating couplers for SiNx waveguides that is simple to fabricate. A numerically optimized uniform grating design is first designed and further optimized by means of a altering the grating height and fill factor to create a final design that yielded a maximum 1dB optical bandwidth of 28.57 nm and a maximum coupling efficiency of 49.77%. The fabrication process requires only one lithography step, and all layers are pre-deposited and etched in one self-aligned process. No surface polishing,

subwavelength mirrors, overlaying, apodization, or genetic equations are needed; making it competitive in future practical production. The close consistency between the simulation results of all 3 cases also confirms the robustness of the design.

IX. References

1. Chen, Xia, et al. *Design and Applications of Silicon Waveguide Grating Couplers*, vol. 8266, SPIE, 2012, doi:10.1117/12.907947.

2. Ding, YH, et al. "Fully Etched Apodized Grating Coupler on the SOI Platform with-0.58 dB Coupling Efficiency." *Optics Letters*, vol. 39, no. 18, 2014, pp. 5348-5350.

3. Marchetti, R., Lacava, C., Khokhar, A., Chen, X., Cristiani, I., Richardson, D., … Minzioni, P. (2017). High-efficiency grating-couplers: demonstration of a new design strategy. Sci Rep, 7(1), 16670. https://doi.org/10.1038/s41598-01716505z

4. Markov, P., JG Valentine, and SM Weiss. "Fiber-to-Chip Coupler Designed using an Optical Transformation." *Optics Express*, vol. 20, no. 13, 2012, pp. 14705-14713.

5. Song, Jeong H., et al. "Grating Coupler Design for Reduced Back-Reflections." *IEEE Photonics Technology Letters*, vol. 30, no. 2, 2018, pp. 217-220.

6. Taillaert, D., et al. "Grating Couplers for Coupling between Optical Fibers and Nanophotonic Waveguides." *Japanese Journal of Applied Physics Part 1-Regular Papers Brief Communications & Review Papers*, vol. 45, no. 8A, 2006, pp. 6071-6077.

7. Xu, PF, et al. "High-Efficiency Wideband SiNx-on-SOI Grating Coupler with Low Fabrication Complexity." *Optics Letters*, vol. 42, no. 17, 2017, pp. 3391-3394.
8. Zaoui, Wissem S., et al. "Bridging the Gap between Optical Fibers and Silicon Photonic Integrated Circuits." *Optics Express*, vol. 22, no. 2, 2014, pp. 1277.
9. Zhang, HJ, et al. "Efficient Silicon Nitride Grating Coupler with Distributed Bragg Reflectors."*Optics Express*, vol. 22, no. 18, 2014, pp. 21800-21805

10. Zhe Xiao, Feng Luan, Tsung-Yang Liow, Jing Zhang, and Ping Shum, "Design for broadband high-efficiency grating couplers," Opt. Lett. 37,530-532,(2012)